J|A|C|S
ARTICLES

Published on Web 11/22/2010

NMR Solution Structure of a DNA−Actinomycin D Complex Containing a Non-Hydrogen-Bonding Pair in the Binding Site

Shannen L. Cravens,[†] Alyssa C. Navapanich,[†] Bernhard H. Geierstanger,[‡] Deborah C. Tahmassebi,*[,†] and Tammy J. Dwyer*[,†]

Department of Chemistry and Biochemistry, University of San Diego, San Diego, California 92110, United States, and Genomics Institute of the Novartis Research Institute, 10675 John Jay Hopkins Drive, San Diego, California 92121, United States

Received August 31, 2010; E-mail: tdwyer@sandiego.edu

Abstract: The solution structures of two different DNA duplexes (one containing a G-T mismatched base pair and the other a non-hydrogen-bonding G-F pair, where F is difluorotoluene) in complex with the peptide antibiotic actinomycin D (ActD) are presented. Using ^{1}H, ^{19}F NMR, and molecular dynamics simulations, we show that there are three major differences between the complexes: (1) ActD binds to the GF duplex in an orientation that is flipped 180° relative to its position in the GT duplex; (2) whereas the difluorotoluene moiety takes the typical *anti* glycosidic conformation in the "free" (uncomplexed) GF duplex, it takes the *syn* conformation in the GF:ActD complex; and (3) in GF:ActD, the difluorotoluene moiety is completely unstacked in the helix; however, the guanine of the G-F pair is stacked quite well with the ActD intercalator and the flanking base on the 5′ side. In GT:ActD, the G-T base pair (although pushed into the major groove from the non-Watson−Crick hydrogen-bonding pattern) stacks favorably with the ActD intercalator and the flanking base pair on the 5′ side. The results described here indicate that a sequence-specific DNA binding ligand such as actinomycin D will, indeed, recognize and bind with high affinity to a DNA incorporating a non-natural, non-hydrogen-bonding nucleoside mimic despite the presentation of modified functionality in the binding site.

Introduction

The incorporation of nucleobase analogues into oligodeoxyribonucleotides has provided marvelous tools for the study of structure and stability in the DNA duplex and has afforded singular opportunities to correlate DNA structure and function.[1−27] Nonpolar, non-hydrogen-bonding isosteres, in particular, offer unique opportunities to investigate the dominant factors responsible for duplex structure and stability: base pairing, aromatic base stacking, and solvation.[11,28] NMR spectroscopic studies have been useful in probing the structural implications of non-hydrogen-bonding pairs in the DNA helix, and a number of solution structures of DNA-containing analogues of natural bases have been reported.[15−17,29−33] Importantly, these studies show

[†] University of San Diego.
[‡] Novartis Research Institute.

(1) Schweitzer, B. A.; Kool, E. T. *J. Org. Chem.* **1994**, *59*, 7238–7242.
(2) Schweitzer, B. A.; Kool, E. T. *J. Am. Chem. Soc.* **1995**, *117*, 1863–1872.
(3) Schweitzer, B. A.; Sheils, C. J.; Ren, X.-F.; Chaudhuri, N. C.; Kool, E. T. *Biological Structure and Dynamics*; Adenine Press: Albany, NY, 1996; Vol. 2, pp 209−216.
(4) Johnson, W. T.; Zhang, P.; Bergstrom, D. E. *Nucleic Acids Res.* **1997**, *25*, 559–567.
(5) Guckian, K. M.; Kool, E. T. *Angew. Chem., Int. Ed.* **1998**, *36*, 2825–2828.
(6) Matray, T. J.; Kool, E. T. *J. Am. Chem. Soc.* **1998**, *120*, 6191–6192.
(7) Wang, X.; Houk, K. N. *Chem. Commun.* **1998**, 2631–2632.
(8) Cubero, E.; Laughton, C. A.; Luque, F. J.; Orozco, M. *J. Am. Chem. Soc.* **2000**, *122*, 6891–6899.
(9) Kool, E. T.; Morales, J. C.; Guckian, K. M. *Angew. Chem., Int. Ed.* **2000**, *39*, 990–1009.
(10) Atwell, S.; Meggers, E.; Spraggon, G.; Schultz, P. G. *J. Am. Chem. Soc.* **2001**, *123*, 12364–12367.
(11) Kool, E. T. *Acc. Chem. Res.* **2002**, *35*, 936–943.
(12) Zimmerman, N.; Meggers, E.; Schultz, P. G. *J. Am. Chem. Soc.* **2002**, *124*, 13684–13685.
(13) Benner, S. A. *Acc. Chem. Res.* **2004**, *37*, 784–797.
(14) Hirao, I. *Curr. Opin. Chem. Biol.* **2006**, *10*, 622–627.
(15) Matsuda, S.; Fillo, J. D.; Henry, A. A.; Rai, P.; Wilkens, S. J.; Dwyer, T. J.; Geierstanger, B. H.; Wemmer, D. E.; Schultz, P. G.; Spraggon, G.; Romesberg, F. E. *J. Am. Chem. Soc.* **2007**, *129*, 10466–10473.
(16) Pfaff, D. A.; Clarke, K. M.; Parr, T. A.; Cole, J. M.; Geierstanger, B. H.; Tahmassebi, D. C.; Dwyer, T. J. *J. Am. Chem. Soc.* **2008**, *130*, 4869–4878.
(17) Malyshev, D. A.; Pfaff, D. A.; Ippoliti, S. I.; Hwang, G. T.; Dwyer, T. J.; Romesberg, F. E. *Chem.-Eur. J.* **2010**, DOI: 10.1002/chem.201000959.
(18) Morales, J. C.; Kool, E. T. *Nat. Struct. Biol.* **1998**, *5*, 950–954.
(19) Schofield, M. J.; Brownewell, F. E.; Nayak, S.; Du, C.; Kool, E. T.; Hsieh, P. *J. Biol. Chem.* **2001**, *276*, 45505–45508.
(20) Francis, A. W.; Helquist, S. A.; Kool, E. T.; David, S. S. *J. Am. Chem. Soc.* **2003**, *125*, 16235–16242.
(21) Jung, K.-H.; Marx, A. *Cell. Mol. Life Sci.* **2005**, *62*, 2080–2091.
(22) Kirby, T. W.; DeRose, E. F.; Beard, W. A.; Wilson, S. H. *Biochemistry* **2005**, *44*, 15230–15237.
(23) Nakano, S.; Uotani, Y.; Uenishi, K.; Fujii, M.; Sugimoto, N. *Nucleic Acids Res.* **2005**, *33*, 7111–7119.
(24) Sismour, A. M.; Benner, S. A. *Nucleic Acids Res.* **2005**, *33*, 5640–5646.
(25) Yang, Z.; Sismour, A. M.; Sheng, P.; Puskar, N. L.; Benner, S. A. *Nucleic Acids Res.* **2007**, *35*, 4238–4249.
(26) Hwang, G. T.; Hari, Y.; Romesberg, F. E. *Nucleic Acids Res.* **2009**, *37*, 4757–4763.
(27) Jarchow-Choy, S. K.; Sjuvarsson, E.; Sintim, H. O.; Eriksson, S.; Kool, E. T. *J. Am. Chem. Soc.* **2009**, *131*, 5488–5494.
(28) Kool, E. T. *Biophys. Biomol. Struct.* **2001**, *30*, 1–22.
(29) Guckian, K. M.; Krugh, T. R.; Kool, E. T. *Nat. Struct. Biol.* **1998**, *5*, 954–958.

10.1021/ja107575f

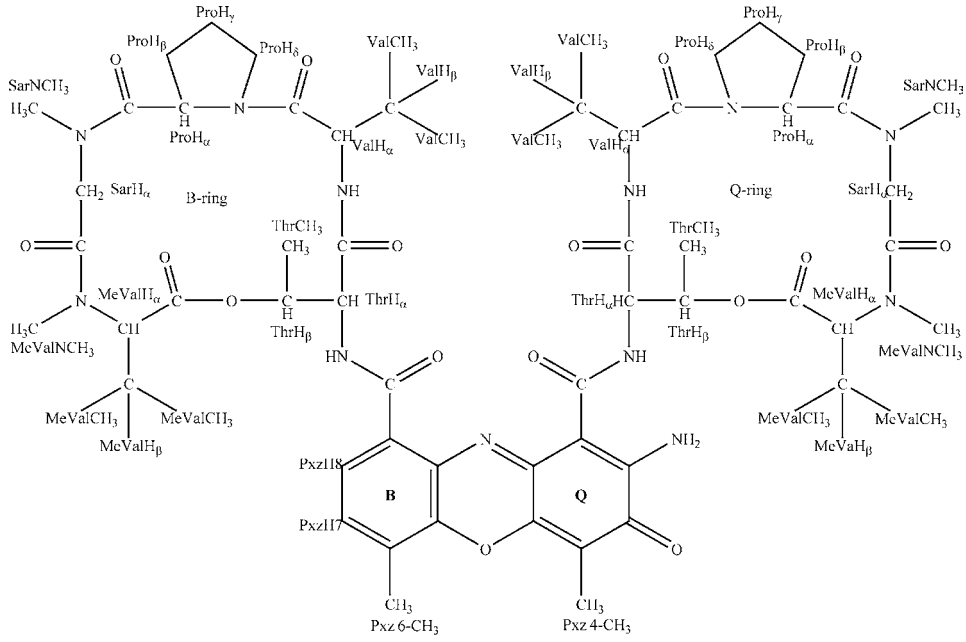

Actinomycin D (**1**)

that, whereas the DNA duplex is destabilized by the inclusion of non-natural nucelobases, global B-DNA structure is retained with minimal localized distortions around the site of modification.

The question remains whether a sequence-specific DNA binding drug will recognize a sequence containing one or more non-natural, non-hydrogen-bonding nucleobases and bind with high affinity. If so, how will the structure of the resulting complex differ from a complex containing natural DNA? Actinomycin D (ActD) is a well-studied antitumor drug (**1**) that binds to DNA by intercalation of its phenoxazone (Pxz) moiety between base pairs via the minor groove. Once bound to the duplex, ActD sterically blocks the progression of RNA polymerase, effectively inhibiting transcription.[34] Early studies on the binding of ActD to DNA sequences demonstrated that the aromatic intercalator has a high specificity for targeting consecutive G·C base pairs and that the two cyclic pentapeptide rings bind in the minor groove, spanning two base pairs on either side of the intercalation site.[35−37] The sequence specificity for G·C steps has been attributed to stabilization via hydrogen bonding between exocyclic guanine amino protons of the target site and the carbonyl oxygens of the ActD threonine residues.[35,38−41] The formation of multiple distinct DNA:ActD complexes with a single binding site is also possible, differing primarily in the orientation of the asymmetric intercalator within the helix.[40,42,43]

More recent studies of DNA:ActD complexes have turned attention to atypical DNA binding sites because ActD has been shown to also bind to duplexes lacking a GpC step.[44−46] Analysis of drug interactions with tandem G-T mismatches in a DNA hairpin has shown that ActD is also capable of binding strongly in the presence of a G·T "wobble pair" in a conformation similar to that of Watson−Crick DNA with localized distortion in the stacking of the bases around the intercalation site.[47] Given these findings, we were curious as to whether a non-natural, non-hydrogen-bonding isostere paired with a natural base would affect the recognition or DNA binding properties of ActD.

We have used ^{1}H, ^{19}F NMR, and molecular dynamics simulations to determine the solution structures of two nearly identical DNA duplexes, each bound with ActD. Both complexes contain a substitution at the GC step in the binding site (5′-AAGCTT-3′). Of the two DNA duplexes studied here, one contains a G-T mismatch (**2**) and the other a G-F pair (**3**), where "F" is difluorotoluene (**4**), a non-hydrogen-bonding isostere of thymine. The complexes are henceforth referred to as GT:ActD and GF:ActD, respectively.

5′-CCAA**G**CTTCC-3′ 5′-CCAA**G**CTTCC-3′
3′-GGTT**T**GAAGG-5′ 3′-GGTT**F**GAAGG-5′
2 **3**

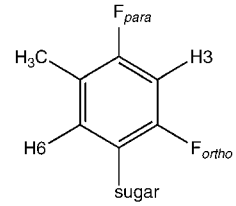

4, "F"

Previous detailed structural analysis[16] of the uncomplexed (or free) decamer DNA duplex **3** revealed that the "F" nucleotide exists in the *anti* conformation about the glycosidic C−C bond, stacks with neighboring bases, and that the absence of hydrogen bonding in the G-F pair likely increases dynamic nucleotide motion. Comparison of free duplex **2** with free duplex **3** showed that the G-F pair exhibits structural features characteristic of both a Watson−Crick pair (on the guanine containing strand) and a mismatch on the strand containing the isostere "F", as evidenced by the helix parameter λ (the angle formed by the glycosidic bond and the cross-strand C1′−C1′ vector). We detail here the recognition of duplexes **2** and **3** by ActD, its relative orientations in the resulting GT:ActD and GF:ActD complexes, and the structural ramifications of drug binding. We believe this represents the first example of ActD binding to a DNA duplex containing a non-natural, non-hydrogen-bonding nucleobase analogue.

Materials and Methods

Sample Preparation. The oligomers d(CCAAGCTTCC), d(GGAAGTTTGG), and d(GGAAGFTTGG) were synthesized and purified by HPLC at Isis Pharmaceuticals, Inc. (San Diego, CA).

Oligomer concentrations, duplex formation, and NMR samples of DNA duplexes **2** and **3** (2 mM) were identical to those described previously.[16] The following numbering system is used to describe the duplexes in these studies:

```
5'- C1  C2  A3  A4   G5   C6  T7  T8  C9  C10 -3'
3'- G20 G19 T18 T17 T/F16 G15 A14 A13 G12 G11 -5'
```

Formation of the 1:1 GT:ActD and 1:1 GF:ActD complexes was followed by NMR. 1D spectra of each duplex sample were acquired on a Varian Inova 500 MHz spectrometer after each addition of approximately 0.25 mol equiv of actinomycin D in CD_3OD solution. Spectra were acquired at 25 °C using 16 382 complex points, 64 scans, and a spectral width of 5913 Hz.

NMR Spectroscopy. ^{1}H NOESY and DQF-COSY spectra were acquired for each complex in D_2O on a Varian Inova 500 MHz spectrometer using the TPPI method of phase cycling.[48] To resolve cross peak overlap, data were collected at 30 °C (GT:ActD) and 25 °C (GF:ActD). Signal assignments for each complex were made using NOESY spectra with a mixing time of 300 ms, spectral width of 5913 Hz, 2048 complex points in t_2 and 512 t_1 increments (zero filled to 2048 on processing). A total of 64 scans were averaged using a recycle delay of 2 s for each t_1 value. Presaturation was applied during the recycle delay and mixing time to suppress residual water signal. Signal assignments were also confirmed using DQF-COSY spectra collected using the same parameters as the NOESY spectra. All spectra for both complexes were processed with Felix (FelixNMR).

All structural restraints were derived using NOESY spectra in D_2O that were acquired using the TPPI method on a Varian Inova 500 MHz spectrometer. Spectra for quantitative analyses of GT:ActD were collected at 30 °C with mixing times of 200 and 50 ms and for GF:ActD at 25 °C with mixing times of 200 and 100 ms (2048 complex points in t_2, 512 t_1 experiments zero filled to 2048 on processing, spectral width of 5913 Hz, and 64 scans for each t_1 value were averaged using a recycle delay of 4 s with presaturation of the HOD resonance). The 2D spectra were apodized with a skewed sine bell function in both dimensions (512 points, phase 60°, skew 0.5−0.7 in t_1; 800 points, phase 60°, skew 0.5−0.7 in t_2). Prior to Fourier transformation in t_1, the first row of the data matrix was multiplied by a factor of 0.5 to suppress t_1 ridges. ^{1}H−^{1}H NOESY in H_2O and ^{1}H−^{19}F NOESY spectra were acquired as described previously.[16,49]

For generating proton distance constraints, the assigned cross peaks of the NOESY spectra were integrated manually using Felix, creating two peak intensity sets for each complex. The NOEs (uncertainties ±20%) were then converted into distances (uncertainties ±0.5 Å) classified as very strong (1.8−2.2 Å), strong (2.2−2.8 Å), medium (2.8−4.0 Å), weak (4.0−4.5 Å), or very weak (4.5−5.0 Å) relative to the intensity of the cytosine H5−H6 cross peak, which is known to be a distance of 2.50 Å. The lower bounds for all distance restraints were set at 1.8 Å. Dihedral torsion angles (uncertainties ±2°) for each complex were loosely restrained based upon close inspection of the C1′H to C2′H/C2″H region (approximately 5.0−6.4 ppm in F1 and 1.8−2.9 ppm in F2) of the DQF-COSY spectra.[50−52] The δ torsion angle was restrained between 110° and 170° for each nucleotide that had a set of antiphase multiplet COSY peaks. The overlap of chemical shifts in the GF:ActD complex hindered detailed analysis of the DQF-COSY spectrum; thus, the δ torsion angles for all nucleotides were loosely restrained between 110° and 170° with a lower force constant than that used for the GT:ActD complex. The use of hydrogen-bonding restraints (uncertainties ±0.2 Å) in our molecular dynamics simulations was justified on the basis of the NMR spectra of the imino protons acquired at 20 °C for both complexes in H_2O. All DNA bases in both complexes, with the exception of difluorotoluene in GF:ActD, had observable imino N−H proton peaks and displayed broadening behavior that is characteristic of Watson−Crick hydrogen-bonded base pairing as temperature increased. A total of 338 constraints were applied to GT:ActD (including Watson−Crick hydrogen-bonding constraints, 264 NMR-derived distance and torsion restraints). For GF:ActD, a total of 448 constraints were applied (including Watson−Crick hydrogen-bonding constraints, excluding the G-F pair, 245 NMR-derived distance and torsion restraints).

Molecular Dynamics Calculations. The solution structures of both complexes were calculated using methods previously described.[16] All forcefield parameters for difluorotoluene and ActD were calculated using Gaussian 98.[53] The SANDER module of AMBER10[54] was used to perform all computational analyses, including energy minimization and restrained molecular dynamics (rMD) calculations. A set of 20 (GT:ActD) and 25 (GF:ActD) initial structures were made by modifying the refined structures of a free GT and GF DNA duplexes with identical sequences.[16] The strands in each duplex starting structure were manually separated by 13−15 Å, and a model of ActD[55] was positioned in the orientation suggested by the NMR analysis. The starting complex structures were then produced following 1000 steps of steepest descent energy minimization using hydrogen-bonding restraints with a force constant of 100 kcal mol^{-1} Å^{-2} and intermolecular NMR restraints with a force constant of 32 kcal mol^{-1} Å^{-2}, followed by slow equilibration to 0 K. Both sets of structures were then subjected to two rounds of restrained simulated annealing. In the first round, the temperature was increased gradually from 0 to 600 K over 5 ps and lowered back to 0 K over the next 15 ps, while all 338 constraints (GT:ActD) or 448 constraints (GF:ActD) were increased over 3 ps to full strength, where they remained for an additional

(30) Guckian, K. M.; Krugh, T. R.; Kool, E. T. *J. Am. Chem. Soc.* **2000**, *122*, 6841–6847.
(31) Klewer, D. A.; Hoskins, A.; Zhang, P.; Davisson, V. J.; Bergstrom, D. E.; LiWang, A. C. *Nucleic Acids Res.* **2000**, *28*, 4514–4522.
(32) Lynch, S. R.; Lu, H.; Gao, J.; Kool, E. T. *J. Am. Chem. Soc.* **2006**, *128*, 14701–14711.
(33) Gallego, J.; Loakes, D. *Nucleic Acids Res.* **2007**, *35*, 2904–2912.
(34) Muller, W.; Crothers, D. M. *J. Mol. Biol.* **1968**, *35*, 251–90.
(35) Jain, S. C.; Sobell, H. M. *J. Mol. Biol.* **1972**, *68*, 1–20.
(36) Lane, M. J.; Dabrowiak, J. C.; Vournakis, J. N. *Proc. Natl. Acad. Sci. U.S.A.* **1983**, *80*, 3260–3264.
(37) Fox, K. R.; Waring, M. J. *Nucleic Acids Res.* **1984**, *12*, 9271–9285.
(38) Sobell, H. M.; Jain, S. C. *J. Mol. Biol.* **1972**, *68*, 21–32.
(39) Liu, X.; Chen, H.; Patel, D. J. *J. Biomol. NMR* **1991**, *1*, 323–347.
(40) Brown, D. R.; Kurz, M.; Kearns, D. R.; Hsu, V. L. *Biochemistry* **1994**, *33*, 651–664.
(41) Gallego, J.; Ortiz, A. R.; de Pascual-Teresa, B.; Gago, F. *J. Comput.-Aided Mol. Des.* **1997**, *11*, 114–128.
(42) Jones, R. L.; Scott, E. V.; Zon, G.; Marzilli, L. G. *Biochemistry* **1988**, *27*, 6021–6026.
(43) Zhou, N.; James, T. L.; Shafer, R. H. *Biochemistry* **1989**, *28*, 5231–5239.
(44) Rill, R. L.; Marsch, G. A.; Graves, D. E. *J. Biomol. Struct. Dyn.* **1989**, *7*, 591–605.
(45) Snyder, J. G.; Hartman, N. G.; D'Estantoit, B. L.; Kennard, O.; Remeta, D. P.; Breslauer, K. J. *Proc. Natl. Acad. Sci. U.S.A.* **1989**, *86*, 3968–3972.
(46) Bailey, S. A.; Graves, D. E.; Rill, R. *Biochemistry* **1994**, *33*, 11493–11500.
(47) Chin, K.-H.; Chen, F.-M.; Chou, S.-H. *Nucleic Acids Res.* **2003**, 2622–2629.
(48) Drobny, G.; Pines, A.; Sinton, S.; Weitekamp, D. P.; Wemmer, D. E. *Faraday Div. Chem. Soc. Symp.* **1979**, *13*, 49–174.
(49) Scott, L. G.; Geierstanger, B. H.; Williamson, J. R.; Hennig, M. *J. Am. Chem. Soc.* **2004**, *126*, 11776–11777.
(50) Baleja, J. D.; Pon, R. T.; Sykes, B. D. *Biochemistry* **1990**, *29*, 4828–4839.
(51) Clore, G. M.; Oschkinat, H.; McLaughlin, L. W.; Benesler, F.; Happ, C. S.; Happ, E.; Gronenborn, A. M. *Biochemistry* **1988**, *27*, 4185–4197.
(52) Gronenborn, A. M.; Clore, G. M. *Biochemistry* **1989**, *28*, 5978–5984.
(53) Pople, J. A.; et al. *Gaussian 98*; Gaussian, Inc.: Pittsburgh, PA, 1998.
(54) Case, D. A.; et al. *AMBER 10*; University of California, San Francisco, CA, 2006.
(55) Lian, C.; Robinson, H.; Wang, A.H.-J. *J. Am. Chem. Soc.* **1996**, *118*, 8791–8801.

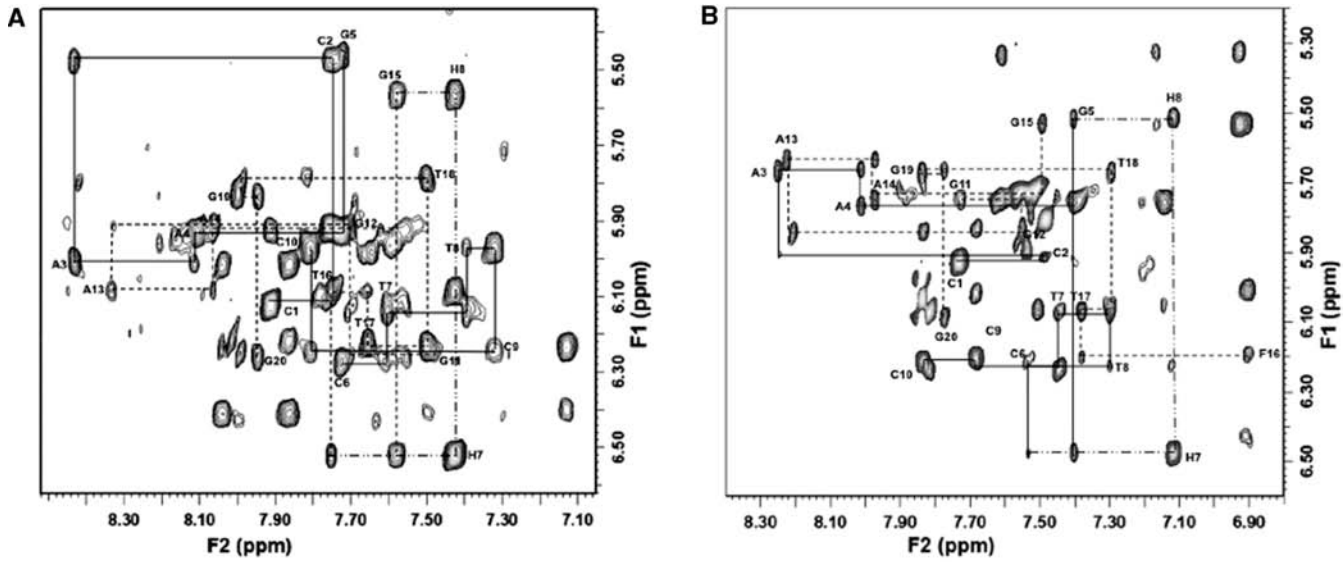

Figure 1. Aromatic to deoxyribose H1′ region of the 300 ms NOESY spectrum of GT:ActD (A) at 30 °C and GF:ActD (B) at 25 °C. Sequential connectivity for residues 1−10 is indicated by a solid line, and residues 11−20 are indicated by a dashed line. The labels designate the H8 to H1′ or H6 to H1′ intranucleotide NOE for each residue; NOEs corresponding to drug resonances are indicated with asterisks.

17 ps of rMD. The refinements were completed with a final cycle of rMD with the same conditions as the first. In each 20 ps round of simulated annealing, the force constant for all NMR-derived distance constraints was increased linearly from 0 to 32 kcal mol^{-1} Å^2 over 3 ps, remaining at 32 kcal mol^{-1} Å^{-2} for the final 17 ps. The force constants for Watson−Crick hydrogen bonding were held constant at 32.0 kcal mol^{-1} Å^{-2} for both rounds. The force constants for the torsion restraints were held constant at 20 kcal mol^{-1} Å^{-2} (GT:ActD) and 15 kcal mol^{-1} Å^{-2} (GF:ActD) for both rounds. Helical parameters for the final structures for both complexes were then determined using CURVES 5.1.[56]

Results

DNA Proton Assignments. Signal assignments of all exchangeable and nonexchangeable nucleic acid protons of the GT:ActD and GF:ActD complexes (with the exception of C5′H and C5″H) were made on the basis of standard procedures.[57,58] Imino N−H protons in both complexes were visible at 10 °C, although the peaks corresponding to G11, G19, and all thymine NH's of GF:ActD were quite broad at this temperature. All imino, amino, and adenine H2 proton assignments for both GT:ActD and GF:ActD were confirmed using ^{1}H NOESY spectra acquired at 10 °C in H_2O (data not shown).

Figure 1 shows the sequential assignment of the aromatic base protons (H6/H8) and the C1′H of the DNA sequence in GT:ActD (30 °C) and GF:ActD (25 °C) in the NOESY spectrum collected in D_2O. Sequential connectivity was also observed for the aromatic protons with C2′H and C2″H of the deoxyribose rings. The absence of intermolecular NOEs at the G5−C6 and G15−T16 steps (GT:ActD) and at the G5−C6 and G15−F16 steps (GF:ActD) in the aromatic to C1′H region suggested the intercalation of ActD at similar sites in both complexes. The downfield shift for H6 of T16 of the mispair as compared to that of free DNA[16] provided additional evidence for the intercalation of ActD at this site for the GT:ActD complex. The C1′H, C2′H, and C2″H assignments were confirmed using cross peaks for C1′H−C2′H and C1′H−C2″H in the DQF-COSY spectra. Other regions of the NOESY spectra were analyzed to determine the deoxyribose ring proton assignments in the complexes. The NOESY and DQF-COSY spectra support one predominant form of both GT:ActD and GF:ActD in solution. Further, in the predominant complex for GF:ActD, the difluorotoluene nucleotide F16, takes the *syn* glycosidic conformation. In contrast to the same region in the NOESY spectrum of the uncomplexed GF-containing[16] duplex in which the intranucleotide NOE for H6−H1′ is extremely weak (indeed, missing at 300 ms), Figure 1 clearly shows a cross peak (much stronger NOE, under similar conditions) for this contact in GF:ActD. These data provide support for the *syn* geometry about the C−glycosidic bond of F16 leading to a shorter distance between the aromatic H6 and deoxyribose H1′ protons. A summary of all DNA assignments for both complexes is listed in the Supporting Information.

The heteronuclear ^{1}H−^{19}F NOESY spectrum (Supporting Information) of the GF:ActD complex permitted the assignment of the two fluorine resonances of F16: The ortho fluorine signal is observed at −123.7 ppm, while the para fluorine signal has a chemical shift of −112.3 ppm. Multiple fluorine signals suggested small amounts of at least one minor form (<20%) in solution. The resonance for the ortho fluorine is broader than that for the para fluorine, consistent with what is observed in the uncomplexed GF duplex,[16] and suggests dynamic motion in difluorotoluene is maintained upon intercalation of ActD. Further inspection of the ^{1}H−^{19}F NOESY spectrum revealed the absence of any NOE between either fluorine atom of F16 and the imino protons of any surrounding bases. This observation is consistent with a *syn* glycosidic conformation for F16 and displacement of the non-natural isostere into the major groove upon drug binding.

ActD Proton Assignments. ActD consists of two cyclic pentapeptide moieties (with the identical sequence (L-Thr)−(D-Val)−(L-Pro)−(Sar)−(L-meVal)) designated as Q-ring and B-ring covalently linked to the quinonoid and benzenoid rings of the phenoxazone intercalator. The asymmetry of the inter-

(56) Lavery, R.; Sklenar, H. *J. Biomol. Struct. Dyn.* **1988**, *6*, 63–91.
(57) Hare, D. R.; Wemmer, D. E.; Chou, S.-H.; Drobny, G.; Reid, B. R. *J. Mol. Biol.* **1983**, *171*, 319–336.
(58) Wuthrich, K. *NMR of Proteins and Nucleic Acids*; John Wiley and Sons: New York, 1986.

Table 1. Proton Chemical Shifts (ppm) for Actinomycin D in GT:ActD and GF:ActD Complexes (One Drug per Duplex)

GT:ActD					GF:ActD		
intercalator	quinonoid (Q)	benzenoid (B)	residue	position	intercalator	quinonoid (Q)	benzenoid (B)
7.43			Pxz	H8	7.14		
6.52				H7	6.57		
1.95				6-CH_3	1.88		
1.68				4-CH_3	1.72		
	4.75	4.84	L-Thr	α		4.52	4.57
	5.46	5.35		*β*		5.18	5.23
	1.48	1.54		CH_3		1.38	1.40
	7.60	7.87		NH		7.78	7.66
	3.77	3.81	D-Val	α		3.55	3.67
	2.31	2.29		*β*		2.12	2.15
	0.97, 1.20	0.98, 1.21		CH_3		0.83, 1.05	0.86, 1.08
	8.20	8.04		NH		8.07	8.10
	6.31	6.42	L-Pro	α		6.24	6.36
	2.12, 3.06	2.19, 3.13		*β*		2.27, 2.86	2.13, 2.99
	2.85, 4.06	2.57, 4.04		*γ*		2.53, 4.10	2.55, 3.87
	2.23, 2.11	1.95, 2.21		*δ*		1.81, 2.13	1.95, 2.27
	4.34, 4.60	4.28, 4.47	Sar	α		4.24, 4.53	4.28, 4.54
	3.06	3.13		NCH_3		2.96	2.98
	2.86	2.88	L-MeVal	α		2.86	2.88
	2.65	2.60		*β*		2.6	2.53
	1.01, 1.07	0.88, 1.05		CH_3		0.91, 1.08	0.88, 0.90
	2.90	2.99		NCH_3		2.84	2.90

Table 2. Intermolecular Drug:DNA NOEs for GT:ActD and GF:ActD

cross peak[a]	GT		ActD		GF		ActD	
1	G5	H8	Pxz	H4CH_3	G5	H8	Pxz	H6CH_3
2	G15	H2′	Pxz	H8	G5	H2′	Pxz	H8
3	G15	H2″	Pxz	H8	G5	H2″	Pxz	H8
4	G5	H1′	ThrQ	CH_3	G5	H1′	ThrB	CH_3
5	G5	H1′	meValQ	Hα	G5	H1′	meValB	Hα
6	G15	H1′	Pxz	H8	G5	H1′	Pxz	H8
7	G15	H8	Pxz	H7	G5	H8	Pxz	H7
	G5	H1′	meValQ	NCH_3				
	G5	H4′	ThrQ	CH_3	G5	H4′	ThrB	CH_3
	G5	H2″	ThrQ	CH_3	G5	H2″	ThrB	CH_3
	T16	H6	Pxz	H6CH_3				
	C6	H5	Pxz	H4CH_3	F16	H6	Pxz	H4CH_3
	G15	H8	Pxz	H8	G5	H8	Pxz	H8
	T16	H4′	Pxz	H8	C6	H4′	Pxz	H8

[a] Cross peak numbering scheme corresponds to labeled peaks in Figure 3.

calator in ActD produces small but distinct differences in the chemical shifts of the similar protons in the two pentapeptide rings. Complete assignments of all nonexchangeable peptide protons in each complex were made by analysis of standard sequential connectivity within each ring, such as those between the H^{α} protons of the Pro, Val, and Sar residues, using NOESY spectra acquired in D_2O.[39,40] The DQF-COSY spectra of the complexes were used to verify any through-bond coupling. Assignment of the exchangeable L-Thr and D-Val NH protons was made using NOESY spectra collected in H_2O via contact with the L-Thr H^{α} protons. The nonexchangeable 6-CH_3, H7, and H8 protons of the benzenoid ring of the intercalator are readily determined by the presence of NOE cross peaks between H7 and H8 and between 6-CH_3 and H7 in the D_2O spectra. Complete proton assignments for the intercalator and cyclic pentapeptide rings for each complex are summarized in Table 1.

Orientation of Drug in GT:ActD and GF:ActD Complexes.

Intercalator in GT:ActD. A total of 31 intermolecular drug−DNA contacts were assigned in the NOESY spectrum to determine the orientation of ActD relative to the DNA sequence in GT:ActD. A complete list of the intermolecular NOEs is given in Table 2. The orientation of the intercalator of ActD in the binding site of the DNA duplex was determined from NOEs observed between the aromatic H7 and H8 protons of the intercalator and the surrounding base pairs. In the GT:ActD complex, several NOEs were observed between the H7 and H8 protons of ActD with G15 and T16 (Table 2). Complementary to these findings was the identification of NOEs between the 4-CH_3 of the quinonoid ring and G5 (Figure 2A). The majority of the intermolecular contacts are concentrated between the Q-ring and G5 and T16 and between the B-ring and G15 and C6. These intermolecular NOEs unambiguously identify the intercalation of the phenoxazone intercalator at the (G5−C6)/(G15−T16) mismatch site for the GT:ActD complex. The data also provide evidence that the intercalator is oriented with the benzenoid ring positioned between G15 and T16 on one strand and the quinonoid ring is between G5 and C6 on the opposite strand.

Intercalator in GF:ActD. A total of 19 intermolecular drug−DNA contacts were assigned in the NOESY spectrum to determine the orientation of ActD relative to the DNA sequence

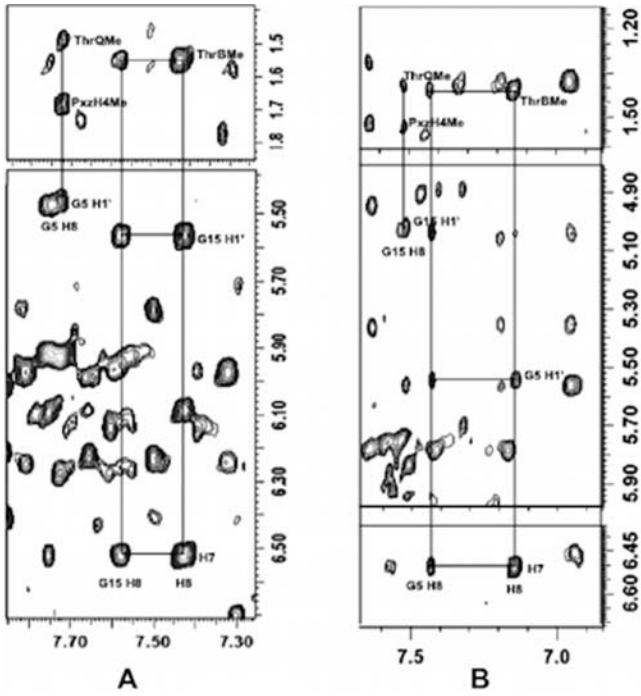

Figure 2. Expanded NOESY (in D_2O) contour plots of GT:ActD (A) at 30 °C and GF:ActD (B) at 25 °C displaying intermolecular connectivity of the intercalator of ActD and the nucleotides of the binding sites. Contacts between the H7 and H8 protons of the intercalator and G15 (GT:ActD) or G5 (GF:ActD) suggest different orientations of the phenoxazone core of ActD within the two duplexes.

in GF:ActD. NOEs were observed between the H7 and H8 protons of ActD with G5 and C6 of the DNA in the predominant form of the complex (Table 2). NOEs were also detected between the 4-CH_3 of the quinonoid ring and G15 (Figure 2B). The intermolecular contacts are concentrated between the Q-ring and G15 and C6 and between the B-ring and G5, with a notable absence of contacts with F16. These intermolecular NOEs unambiguously identify the site of the phenoxazone intercalator at the (G5−C6)/(G15−F16) mismatch site for the GF:ActD complex. The intercalator is flipped 180° relative to the orientation within the GT:ActD complex such that the benzenoid ring is positioned between G5 and C6 on one strand and the quinonoid ring is between G15 and F16 on the opposite strand. No NOEs were detected between the H7 and H8 protons of the intercalator and any other nucleotides in GF:ActD, suggesting that ActD is bound in a similar fashion in any minor form of the complex. Because of the overlap of chemical shifts caused by the similarities between the major and minor forms, no other structural details for the minor form could be gleaned from the NMR data collected. We suspect that the differences between the two forms are localized to the region of the G-F pair in the duplex.

Peptide Rings in GT:ActD and GF:ActD. The orientations of the pentapeptide rings relative to the DNA sequences were determined by intermolecular NOEs between the amino acid protons of the Q-ring and B-ring with the minor groove base and sugar protons of the nucleotides in and around the binding site. On the Q-ring, the L-Thr protons exhibit NOEs to G5 (GT:ActD) or G15 (GF:ActD), whereas L-Pro protons exhibited NOEs to T16 and T17 (GT:ActD) or C6 and T7 (GF:ActD). The Sar protons exhibit NOEs to T17 and T18 (GT:ActD) or T7 and T8 (GF:ActD), whereas the L-meVal protons exhibit NOEs to G5 (GT:ActD) or G15 (GF:ActD). The Sar protons exhibit NOEs to T7 and T8 (GT:ActD) or T17 and T18 (GF:ActD), whereas the L-meVal protons exhibit NOEs to G15 (GT:ActD) or G5 (GF:ActD). On the B-ring, the L-Thr protons exhibit NOEs to G15 (GT:ActD) or G5 (GF:ActD), whereas L-Pro protons of the Q-ring exhibited NOEs to C6 and T7 (GT:ActD) or T17 with no detectable contact with F16 (GF:ActD). In summary, both the quinonoid and the benzenoid pentapeptide rings are positioned in the minor groove of the DNA in each complex and span two base pairs on either side of the intercalation site. The disparity in the nucleotides that the pentapeptide rings contact in both complexes is a consequence of the different orientations of the phenoxazone intercalator. A comparison of the contacts between G15 (GT:ActD) or G5 (GF:ActD) with various residues of ActD verifies that the guanine residue positioned above the benzenoid ring of the intercalator is oriented similarly in both complexes (Figure 3 and Table 2).

As compared to GT:ActD, for which a number of intermolecular contacts between T16 and ActD exist, we can identify no NOEs between F16 and the pentapeptide rings of ActD. This suggests an enhanced displacement of F16 into the major groove of the duplex relative to the displacement of thymine in a G-T mismatch,[16] eliminating close contact between the isostere and the pentapeptide rings of the drug. However, we do observe a relatively strong NOE between the F16 methyl and the 6-CH_3 of the intercalator. This contact suggests the glycosidic angle of the non-natural nucleotide is in the *syn* conformation rather than the *anti* conformation that is most commonly observed in Watson−Crick DNA (and retained in the free GF duplex[16]). It could be that the *syn* conformation provides additional opportunity for the F16 methyl group to form favorable van der Waals interactions with the intercalator of the drug.

Quality of the Structures. The families of structures used to represent each complex were generated using statistical analysis modeled after Smith et al.[59] The structures resulting from rMD for each complex were randomly ordered, and the mean all-atom pairwise rmsd was calculated for the first two structures, then the first three structures, etc. This process was repeated 500 times with each round using a different ordering of the structures. This analysis predicts the minimum number of structures necessary to fully represent the conformational space consistent with the experimental data. It was determined that 12 structures (GT:ActD) and 15 structures (GF:ActD) were sufficient to describe the complexes. The structures in each family were chosen to minimize the molecular mechanics (AMBER) energy and the constraint violation energy. The superposition of the family of structures describing both complexes is shown in Figure 4 along with the average structures for the complexes and the binding sites.

The energy and rmsd characteristics of the ensembles of structures for GT:ActD and GF:ActD are summarized in Table 3. The data indicate structural convergence for the GT:ActD complex with an rmsd of 0.94 Å (rms difference from the mean structure of 0.64 Å) and for the GF:ActD complex with an rmsd of 1.36 Å (rms difference from the mean structure of 0.93 Å), given that the starting structures for both complexes represented a range of B-DNA conformations with strands separated between 13 and 15 Å and initial rmsd values of 3.95 Å (GT:ActD) and 4.82 Å (GF:ActD). The complexes were annealed through restrained minimization, resulting in structures with rmsd values of 2.06 Å (GT:ActD) and 2.05 Å (GF:ActD). The

(59) Smith, J. A.; Gomez-Paloma, L.; Case, D. A.; Chazin, W. J. *Magn. Reson. Chem.* **1996**, *34*, S147–S155.

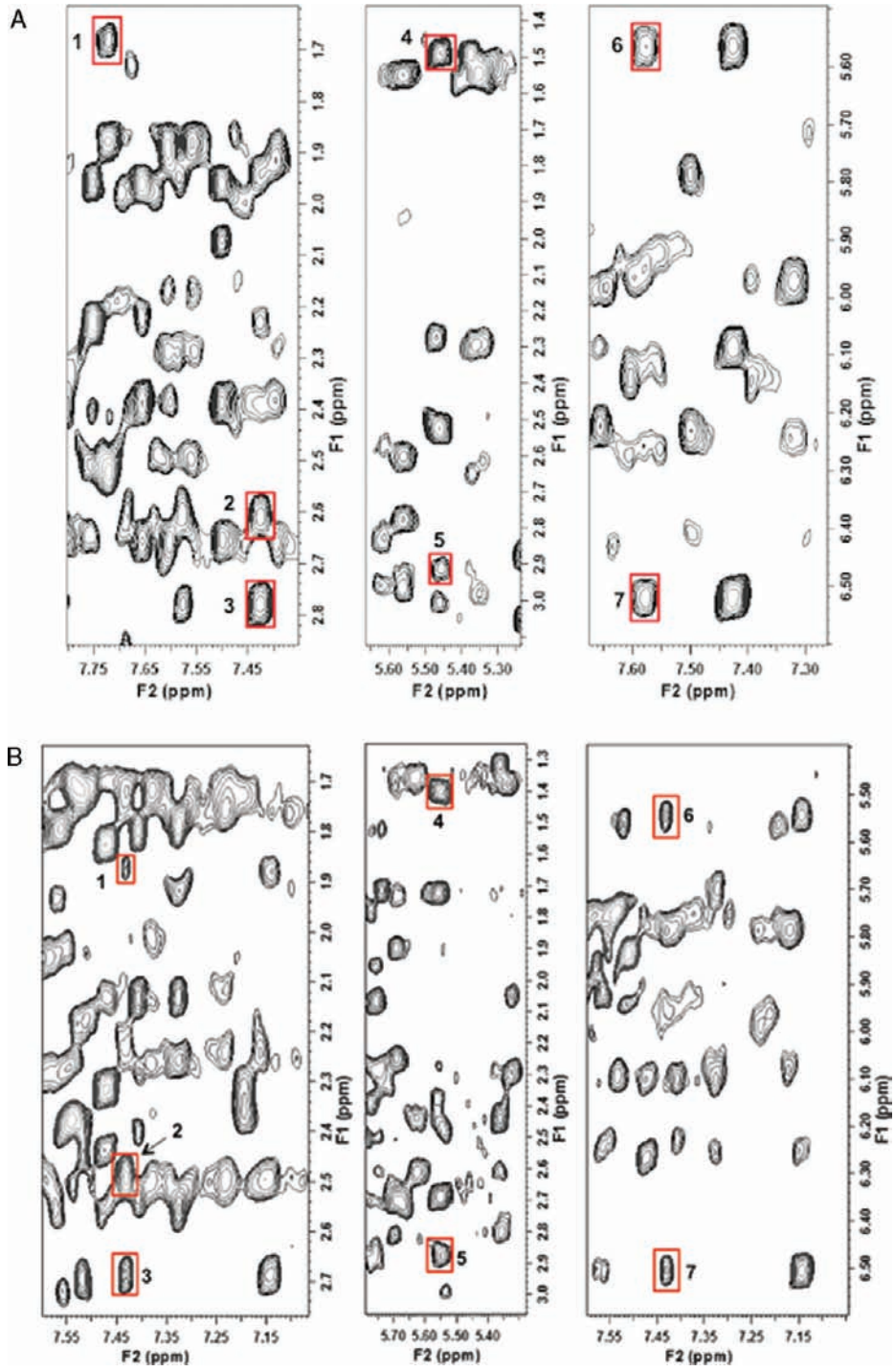

Figure 3. Expanded NOESY contour plots of GT:ActD (A) and GF:ActD (B) in D_2O at 30 and 25 °C, respectively, displaying intermolecular connectivity of the intercalator of ActD and the nucleotides of the binding sites. The numbers used to label key cross peaks correspond to those given in Table 2.

central six base pairs for each complex showed greater convergence in structure, as is also seen in Table 3. The final collection of structures have a total restraint violation summing to 9.6 ± 0.8 kcal for GT:ActD and 6.9 ± 1.4 kcal for GF:ActD, amounting to 0.2% (GT:ActD) and 0.1% (GF:ActD) of the total energy of each system.

Structural Features of the Complexes. GT:ActD. The average solution structure describing the GT:ActD complex is shown in Figure 4B. Closer inspection of the intercalation site illuminates the stacking interactions between the DNA and ActD (Figure 5A). The G5•T16 and C6•G15 base pairs flank the ActD phenoxazone core with G5 stacking with the quinonoid ring. T16 is displaced considerably into the major groove of the helix (due to hydrogen bonding in the mismatch), prohibiting effective stacking with the intercalator.

GF:ActD. The average solution structure describing the GF:ActD complex is shown in Figure 4E. Comparison of the intercalation site with that of GT:ActD reveals a distinct difference in the stacking interactions between the DNA and ActD (Figure 5B). The G5•F16 and C6•G15 pairs of the binding site exhibit atypical stacking interactions in which G5 and G15 are both found to stack nearly on top of the center ring of the

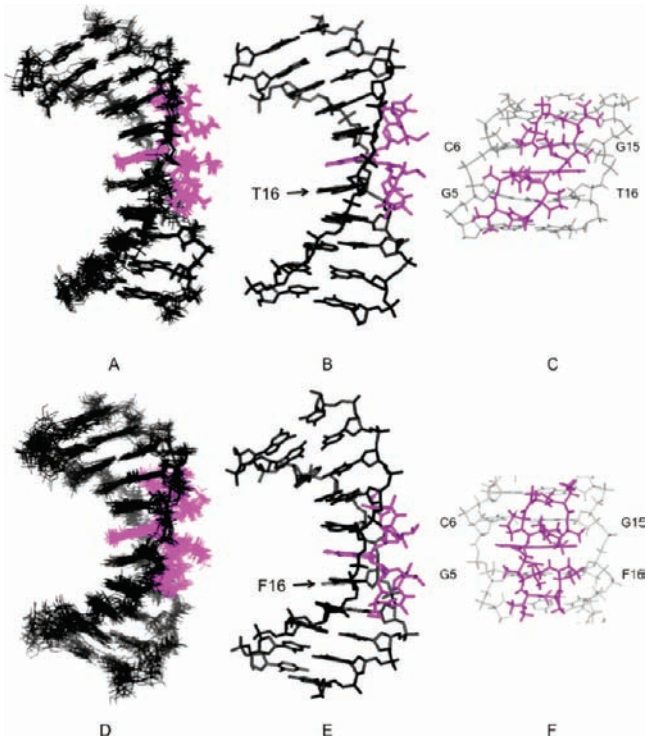

Figure 4. Superposition of the family of 12 structures describing the GT:ActD complex (A), average structure (B), and view into the minor groove (C), derived from rMD; and the superposition of the family of 15 structures describing the GF:ActD complex (D), average structure (E), and view into the minor groove (F).

Table 3. Summary of Energies, rmsd Values, and Violations for Ensembles of Structures

	GT:ActD	GF:ActD
Molecular Mechanics Energies (kcal)		
E_{Amber}	-5142.6 ± 5.9	-5145.5 ± 6.0
E_{Viol}	9.6 ± 0.8	6.9 ± 1.4
Average Pairwise rmsd (Å)		
DNA	0.92	1.57
ActD + DNA	0.94	1.36
ActD + DNA binding site	0.88	1.05
Distance Violations (Å)		
$0.05 < d \leq 0.10$	17	19
$0.10 < d \leq 0.20$	4	0
$0.20 \leq d$	0	0

phenoxazone core. Considerable displacement of difluorotoluene into the major groove of the helix is also observed, far beyond that of a G-T mismatch, completely prohibiting stacking with the intercalator and T17. As mentioned previously, the glycosidic bond in the F16 nucleotide takes on the *syn* conformation. These structural perturbations are attributed to the lack of hydrogen bonding within the G-F pair, likely increasing dynamic motion and flexibility in the binding site as the helix attempts to maximize stabilizing interactions with ActD.

Drug−DNA Hydrogen Bonds. The sequence specificity of ActD has been attributed to the formation of particular intermolecular hydrogen bonds upon intercalation of the drug into the DNA helix. In the GT:ActD complex, the backbone carbonyl groups of L-Thr of the Q-ring and L-Thr of the B-ring are within hydrogen-bonding distance of the NH_2 groups of G5 and G15, respectively. Putatively the L-Thr carbonyl groups of both pentapeptide rings form the same hydrogen bonds in the GF:ActD complex. Weaker hydrogen bonds are likely formed between the backbone amide NH of the L-Thr residues and the N3 of G5 and G15. The majority of the intermolecular hydrogen bonds are at slightly longer distances in GF:ActD than in GT:ActD, and all are somewhat longer in these complexes than those typically observed when ActD binds between two G·C steps.[38−40] Additional hydrogen bonds are also proposed to form between the amino group of the quinonoid ring of the intercalator of ActD and the O4′ of C6 and O3′ of G5 (GT:ActD) or G15 (GF:ActD). Intramolecular hydrogen bonds are observed between the amide proton and carbonyl oxygen of the D-Val residues on opposite pentapeptide rings in both complexes. These interactions help to stabilize the position of the B-ring and Q-ring in the minor groove of the DNA helix.

The existence of interbase hydrogen bonds was evaluated using a series of 1D ^{1}H NMR spectra collected in H_2O as a function of temperature (Supporting Information) as well as 2D NOESY spectra acquired in H_2O. All base pairs in GT:ActD and all except the G-F pair in GF:ActD had observable imino N−H proton peaks and displayed broadening behavior that is characteristic of Watson−Crick hydrogen-bonded base pairing as temperature increased. This suggests that the hydrogen-bonding pattern of the DNA sequence (with the exception of the G-F pair) was not disturbed by the intercalation of ActD.

Helix Parameters. Both the GT:ActD and the GF:ActD complexes exhibit overall B-form DNA geometry with deformations localized to the base pairs having intermolecular contacts with ActD. The terminal nucleotides of each strand display substantial dynamic behavior and a deficiency of NOE data. The helical parameters that characterize both complexes are displayed in Figure 6.

The variation in the buckle of the G5−T16 and C6−G15 base pairs in GT:ActD results from the pronounced tilt of G15, C6, and T16 toward the intercalator as can be seen in Figure 6. The tilt of C6 and T16 has been observed in DNA:ActD complexes containing tandem G-T mispairs in the binding site, and it is presumed to be a result of the displacement of the thymine residue changing the binding surface of the intercalator.[47] G15 exhibits tilting behavior that is not characteristic of guanine bases in the intercalation site, which normally stack directly on top of the phenoxazone ring. This tilt in the binding site is also observed in the GF:ActD complex (between C6 and F16), whereas the guanine residues remain parallel with the intercalator. The large variation in the buckle of the G5−F16 step in GF:ActD can also be attributed to the orientation of the non-natural nucleotide that is displaced into the major groove. The negative shear of the binding site in both complexes also indicates a displacement of the mismatches into the major groove, which is much more pronounced in GF:ActD. F16 also exhibits a large positive inclination of a magnitude that is similar to, but larger in magnitude than, that observed in the free GF duplex. The displacement of the F16 also induces a large variation in the tilt between the A4−T17 and G5−F16 steps to optimize stacking and van der Waals interactions within the binding site.

In GT:ActD, the negative propeller twist of the base pair on the 3′ side of the G-T wobble pair is typical of DNA duplexes containing these mismatches.[60] Unlike the positive propeller twist and opening determined for the free GF duplex, a large negative value for each parameter is observed in GF:ActD. This is attributed to the *syn* glycosidic conformation of the non-

(60) Bhattacharya, P. K.; Cha, J.; Barton, J. K. *Nucleic Acids Res.* **2002**, *30*, 4740–4750.

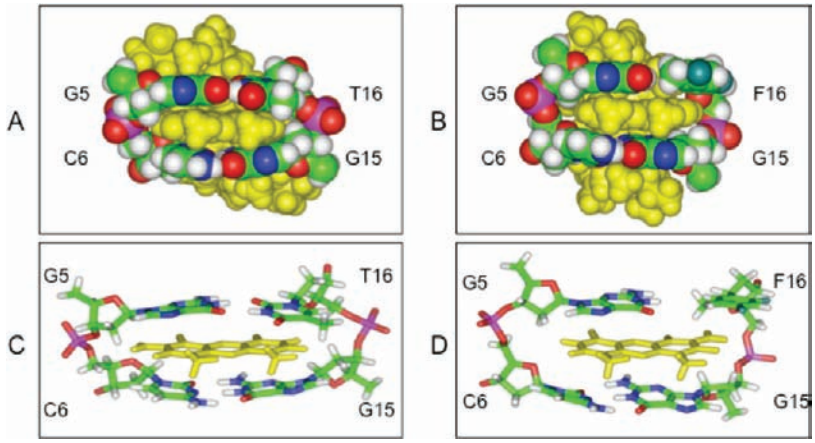

Figure 5. Space-filling models of the GT:ActD (A) and GF:ActD (B) intercalation sites viewed from the major groove. The stacking interactions between the phenoxazone intercalator and the binding sites are displayed for GT:ActD (C) and GF:ActD (D).

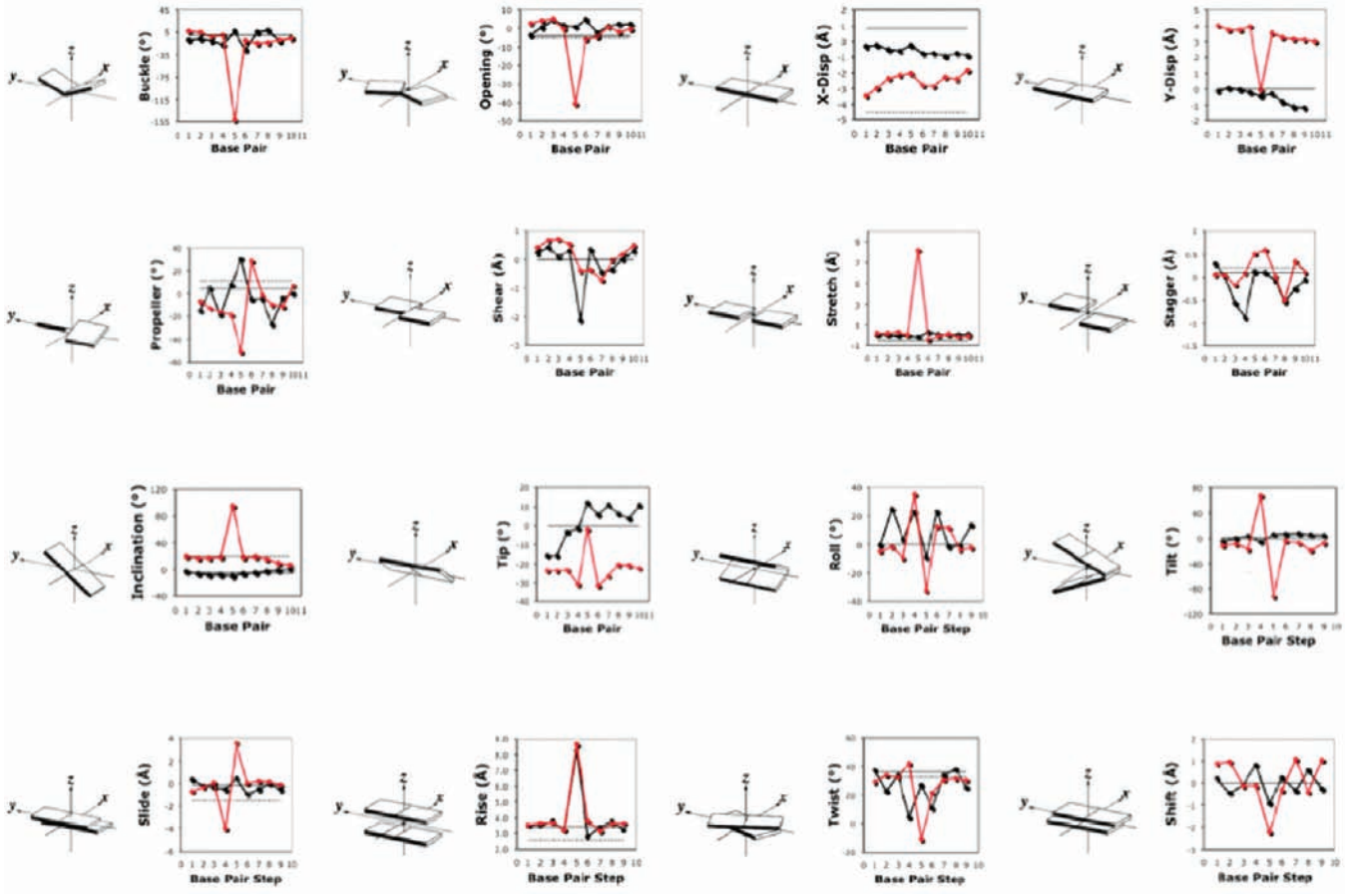

Figure 6. Helical parameters for the GT:ActD (black) and GF:ActD (red) average structures obtained using CURVES. Standard values for canonical B-DNA and A-DNA are indicated by solid and dashed horizontal lines, respectively.

natural nucleotide. The sharp decrease in the twist of GF:ActD between the A4−T17 and G5−F16 steps also results from the *syn* glycosidic angle in F16. The roll at individual steps in both complexes is similar to those observed in other ActD:DNA complexes and results from binding of the pentapeptide rings.[61] Note that the roll is larger in magnitude for GF:ActD than for GT:ActD, suggesting a slightly greater curvature of the GF:ActD complex. As shown in Figures 5 and 6, the significantly larger value of the rise at the intercalation site is attributed to the large gap that forms between the GC and GT/GF steps when the drug is bound. This separation is pronounced in comparison with free DNA[16] and nearly identical in both complexes described here.

The deoxyribose ring conformations have an average pseudorotation phase angle (sugar pucker) of 130° (GT:ActD) and 136° (GF:ActD) with major interruptions localized to the ActD binding site (Figure 7).

Analysis of the helical parameters λ_1 and λ_2 provides further evidence of the localized distortions in the binding site of both the GT:ActD and the GF:ActD complexes. The symbol λ is

(61) Chen, H.; Liu, X.; Patel, D. J. *J. Mol. Biol.* **1996**, *258*, 457–479.

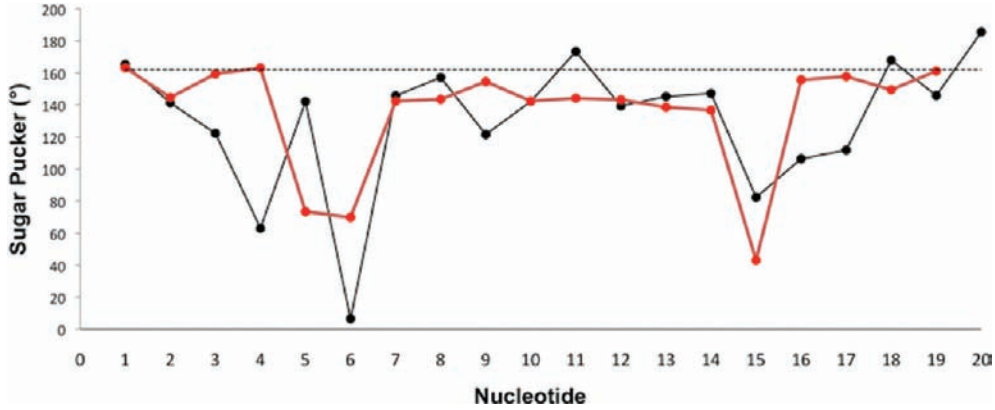

Figure 7. Comparison of the deoxyribose ring conformations in GT:ActD (black) and GF:ActD (red) to the expected values of B-form DNA (dashed horizontal line).

Table 4. Helical Parameters λ_1 and λ_2 for the GT:ActD and GF:ActD Complexes

GT:ActD			GF:ActD		
base pair	λ_1 (deg)	λ_2 (deg)	base pair	λ_1 (deg)	λ_2 (deg)
C1−G20	56 ± 1	52 ± 1	C1−G20	57 ± 2	53 ± 1
C2−G19	58 ± 1	54 ± 1	C2−G19	58 ± 2	54 ± 1
A3−T18	57 ± 2	56 ± 2	A3−T18	59 ± 2	56 ± 2
A4−T17	57 ± 1	56 ± 2	A4−T17	57 ± 2	51 ± 1
G5−T16	45 ± 2	65 ± 1	G5−F16	51 ± 4	81 ± 7
C6−G15	59 ± 1	54 ± 1	C6−G15	55 ± 2	53 ± 1
T7−A14	51 ± 1	56 ± 2	T7−A14	54 ± 1	58 ± 1
T8−A13	52 ± 1	56 ± 1	T8−A13	56 ± 1	58 ± 2
C9−G12	56 ± 1	55 ± 1	C9−G12	59 ± 2	52 ± 1
C10−G11	57 ± 1	54 ± 1	C10−G11	58 ± 1	52 ± 2

used to represent the angle between the glycosidic bond (N1 (pyrimidine) or N9 (purine) to its own C1′) and the C1′−C1′ vector with its complementary nucleotide. Each base pair is characterized by two values of λ: λ_1 is the angle for the strand C1−C10, and λ_2 is the complementary angle for strand G11−G20. Table 4 shows the measured values of λ_1 and λ_2 in the GT:ActD and GF:ActD complexes. The Watson−Crick base pairs of both complexes maintain the symmetry in λ angles observed in the free DNA (nominally 56°). Interestingly, the asymmetry of the G-T mismatch observed in the free GT duplex (41° and 66°)[16] is largely maintained in GT:ActD (45° and 65°). The value of λ for G5 in the GF:ActD complex (51°) is slightly reduced from its value in the free GF duplex (54°),[16] which more closely matched the Watson−Crick value, due to binding of ActD. The larger λ angle for F16 in GF:ActD (81°) relative to "free" GF duplex (70°)[16] is due to displacement of the non-hydrogen-bonding isostere into the major groove.

Discussion

The solution structures of two similar DNA duplexes, one containing a G-T mismatch and the other containing a non-hydrogen-bonding G-F (where F is difluorotoluene) pair, in complex with ActD have been determined by NMR spectroscopy and molecular dynamics simulations. In GT:ActD, binding of the drug via intercalation at the GT/CG step is indicated by intermolecular NOEs placing the benzenoid ring between G15 and T16 on one strand and the quinonoid ring between G5 and C6 on the opposite strand. In GF:ActD, the drug binds via intercalation at the GF/CG step, albeit in an orientation that is flipped by 180° relative to the binding site in GT:ActD, as implied by intermolecular NOEs between the benzenoid ring and G5 and C6 on one strand and the quinonoid ring between G15 and F16 on the opposite strand. In both complexes, the pentapeptide rings lie in the minor groove and span two base pairs on either side of the intercalation site. These findings are consistent with the model of the ActD−d(ATGCAT) complex proposed by Sobell and Jain[38] despite the inclusion of a G-T mismatch or a non-hydrogen-bonding G-F pair in place of one G-C base pair in the binding site.

Thermodynamic measurements[45] and footprinting studies[62] have shown that ActD binds with relatively high affinity to DNA sites containing a central GpC step flanked by A-T base pairs. While some variation in magnitude was reported depending on the precise sequence context, binding sites containing 5′-TGCT-3′ or 5′-TGCA-3′ displayed the highest binding constants of 6.4×10^6 to 1.4×10^7 M^{-1}, whereas ActD binds more weakly to sequences containing a CpG step as the intercalation site (binding constants around 10^5 M^{-1}). DNA sequences that lack a GpC step are known to bind ActD rather poorly with binding constants $<10^4$ M^{-1}. Chin et al.[47] report a remarkably high binding constant of $(8.2 \pm 1.5) \times 10^6$ M^{-1} for ActD with a DNA hairpin-containing tandem G-T mismatches in the unusual binding site 5′-CGTT-3′/3′-TGTG-5′. While we have not measured binding constants in the present study, on the basis of the lack of exchange broadening in the NMR titration data at intermediate ratios of added drug (Supporting Information), we estimate that the overall binding affinity of ActD is nearly as high in the GF:ActD as in GT:ActD.

Results from previous NMR studies of ActD bound to various DNA sequences attribute the specificity of drug binding to a combination of aromatic stacking interactions and hydrogen bonding.[39,40,42,43,47,55,63,64] The displacement of the thymine residue of a G-T mispair into the major groove (to accommodate hydrogen bonding with guanine on the opposite strand) leads to different stacking interactions with adjacent bases than would result from a G-C base pair in the same position. The persistence of the G5 and T16 imino peaks at higher temperatures in the ^{1}H NMR spectra in H_2O implies that hydrogen bonding of the G-T base pair is conserved following the binding of ActD, whereas G5 of GF:ActD shows no evidence of hydrogen bonding to any acceptor group. We previously reported[16] that

(62) Goodisman, J.; Rehfuss, R.; Ward, B.; Dabrowiak, J. C. *Biochemistry* **1992**, *31*, 1046–1058.
(63) Wilson, W. D.; Jones, R. L.; Zon, G.; Scott, E. V.; Banville, D. L.; Marzilli, L. G. *J. Am. Chem. Soc.* **1986**, *108*, 7113–7114.
(64) Chen, F.-M.; Sha, F.; Chin, K.-H.; Chou, S.-H. *Nucleic Acids Res.* **2003**, *31*, 4238–4246.

replacing the thymine of a G-T mispair with a difluorotoluene molecule permits the guanine in the G-F pair to stack with adjacent bases as if it were in a Watson−Crick base pair, whereas the difluorotoluene of the G-F pair occupies a position in the helix that more closely resembles the thymine of a G-T mispair. In the present study, we have shown that ActD does, indeed, recognize and bind with high affinity to a DNA sequence containing a non-hydrogen-bonded pair. The G-C base pairs that flank the intercalator in ActD−d(ATGCAT) complexes exhibit prominent stacking of the phenoxazone ring with guanine residues, but an absence of stacking with cytosine residues.[39] These basic features are also found in the GT:ActD and GF:ActD complexes with effective stacking observed largely between the intercalator and the guanine residues of the binding sites. The intermolecular hydrogen bonds between guanine residues and ActD that are responsible for the binding specificity of ActD are maintained in both the GT:ActD and the GF:ActD complexes. Because the drug is oriented differently by 180° in the two complexes, these stabilizing hydrogen bonds occur with different guanine residues (on opposite strands). We believe these interactions are somewhat weaker than those observed when ActD binds to canonical Watson−Crick DNA, which suggests to us that perturbing the binding site (via incorporating a mismatch or removing interbase pair hydrogen bonding) destabilizes the complex by an unknown amount.

The recognition of mismatched base pairs by DNA repair enzymes is a highly selective and finely tuned process that is essential to sustain biological systems. Kennard and coworkers[65,66] have studied the efficiency of mismatch repair as a function of DNA sequence, structure and mismatch type. One particular helical parameter, λ, appears to correlate well with the efficiency of mismatch repair (and, by extension, recognition). As mentioned above, each base pair is characterized by two values for λ, defined as the angle between the glycosidic bond (N1 (pyrimidine) or N9 (purine) to its own C1′) and the C1′−C1′ vector with its complementary nucleotide. Canonical Watson−Crick base pairs exhibit symmetry with respect to λ_1 and λ_2, each having an average value of approximately 55.9°; however, the λ angles at a mismatch site have markedly asymmetric values.[65−67] The magnitude of asymmetry in λ for various mispairs follows GT > CA > GA and parallels the efficiency of repair.[68−70] In the context of a large oligonucleotide, we posited that a repair enzyme might detect damaged DNA by sensing the deviation from Watson−Crick symmetry of the base pairs reflected in λ.[16] Once recognized, however, we were curious about how the DNA bases would "respond" and whether or not a binding event would significantly alter base pair stacking symmetry as measured by λ. In both GT:ActD and GF:ActD complexes, whereas the Watson−Crick bases of the DNA sequence flanking the intercalation sites maintain symmetry, the λ values for the "damaged" pairs in the binding site demonstrate substantial asymmetry. These results illuminate two important features of DNA structure and function: (1) DNA is remarkably flexible and accommodates stress (such as binding of a small molecule) by localizing structural deformations and recovers fairly canonical structure just beyond the binding site; and (2) the hydrogen-bonding pattern in a base pair defines and fixes the aromatic stacking interactions between the bases and nearby aromatic molecules, whether covalently attached to the DNA or not. In the case of GT:ActD binding, the hydrogen bonding in the G-T base pair (though non-Watson−Crick) confers asymmetric λ angles and provides minimal flexibility for the bases to move relative to one another to improve the stacking with the phenoxazone intercalator. In GF:ActD, however, due to the absence of hydrogen bonding, guanine (G5) and difluorotoluene (F16) in the G-F pair can move independently to establish favorable and stabilizing interactions with nearby groups/bases. Because it is not tethered by hydrogen bonding to the base on the opposite strand, guanine (G5) stacks with the ActD phenoxazone core more effectively than guanine in a G-T mismatch, but less effectively than guanine in a G-C base pair (based on λ values). Likewise, difluorotoluene in the G-F pair of GF:ActD (that, even in the free GF duplex, is less well stacked than the thymine of a G-T mismatch) stacks extremely poorly in the helix (having a λ value of 81°) and with the ActD phenoxazone core. The fact that the glycosidic torsional angle in free GF duplex[16] is in the *anti* conformation whereas we observe it to be *syn* in the GF:ActD complex may be driven by a hydrophobic effect. The F16 methyl group is found to orient into the minor groove where it may enhance the hydrophobic pocket in which the ActD intercalator sits (see Figure 5B). We further speculate that the difference in the shape of the binding pocket for the phenoxazone intercalator when bounded by GT/GC (in GT:ActD) versus GF/GC (in GF:ActD) is responsible for the different orientations observed for ActD in these complexes. Given that stabilizing hydrogen bonds are still able to form between the residues in the peptide rings of ActD that are in close contact with the DNA, regardless of the orientation of the intercalator, drug binding to both sequences with high affinity is achieved.

Acknowledgment. We thank Dr. Jeremy Kua (USD) for helpful discussions, and we thank Joanna Cole, Jeremiah Fillo, Timothy Parr, and Danielle Pfaff for early efforts that contributed to this work. The NMR facility at USD was established with a grant from the NSF-MRI program (0417731). Funding was provided by the Blasker−Rose−Miah Fund at the San Diego Foundation (grant to T.J.D. and D.C.T.).

Supporting Information Available: Complete chemical shift assignments and supporting tables; ^{1}H−^{19}F NOESY spectrum; and imino proton regions of the ^{1}H spectra for GT:ActD and GF:ActD. This material is available free of charge via the Internet at http://pubs.acs.org.

JA107575F

(65) Hunter, W. N.; Brown, T.; Anand, N. N.; Kennard, O. *Nature* **1986**, *320*, 552–555.
(66) Hunter, W. N.; Brown, T.; Kennard, O. *Nucleic Acids Res.* **1987**, *15*, 6589–6606.
(67) Allawi, H. T.; SantaLucia, J., Jr. *Nucleic Acids Res.* **1998**, *26*, 4925–4934.
(68) Fersht, A. R.; Knill-Jones, J. W.; Tsui, W. C. *J. Mol. Biol.* **1982**, *156*, 37–51.
(69) Lu, A. L.; Welsh, K.; Clark, S.; Su, S. S.; Moldrich, P. *Cold Spring Harbor Symp. Quant. Biol.* **1984**, *49*, 589–596.
(70) Kramer, B.; Kramer, W.; Fritz, H. J. *Cell* **1984**, *38*, 879–887.